

## CCD ASTROMETRY. I. PRELIMINARY RESULTS FROM THE KPNO 4-m/CCD PARALLAX PROGRAM

DAVID G. MONET<sup>a)</sup>

Mount Wilson and Las Campanas Observatories, Pasadena, California 91101

CONARD C. DAHN<sup>a)</sup>

U.S. Naval Observatory, P.O. Box 1149, Flagstaff, Arizona 86001

Received 7 March 1983; revised 31 May 1983

### ABSTRACT

A program to measure trigonometric stellar parallaxes using a charge coupled device (CCD) at the prime focus of the Kitt Peak National Observatory (KPNO) 4-m telescope was started in July 1980. Preliminary parallaxes have been measured for 11 stars. The three prime candidates have uncertainties in the mean position of about 1 milliarcsecond and uncertainties in the parallax of about 2 milliarcseconds. This first paper discusses many of the technical aspects of the program and presents these parallaxes.

### I. INTRODUCTION

The primary goal of the KPNO 4-m/CCD parallax program is to measure parallaxes of a selection of faint, astrophysically interesting stars. Because of their faint apparent magnitudes, all but the nearest stars populating the cool end of the main and degenerate sequences are beyond the practical reach of existing photographic parallax programs. For example, the U.S. Naval Observatory program has measured parallaxes for about 30 stars fainter than  $V \cong 16.0$  and of these only two are fainter than  $V \cong 17.0$  (Dahn *et al.* 1982, and references cited therein). Exposure times of an hour or more are required to properly photograph  $V \gtrsim 17.0$  stars with the USNO astrometric reflector. Hence only a handful of these faint stars can be included in the program. Consequently, reliable trigonometric parallaxes have been measured for only five stars with  $M_v \gtrsim 16.5$  (W359, G51-15, L745-46B, vB8, and vB10). Since stars at the faint end of the main sequence (e.g., vB10) have  $M_v \cong 18.0$ , they can be routinely observed only if they are within 6 parsecs. Since high quality modern parallax determinations are reliable (10% errors) to a distance of approximately 30 parsecs, many more intrinsically faint stars could be measured by a program that routinely observes at faint apparent magnitudes. Accurate distances to a substantially larger sample of these low mass stars will contribute significantly to a better understanding of the lower main sequence. A similar incompleteness exists for stars at the faint end of the degenerate sequence. In addition, many stars with faint apparent magnitudes and larger proper motions probably belong to the Galactic halo population, and, in extreme cases,

may be only marginally bound to or even escaping from the Galaxy. Distances to these objects are important for the study of the chemical and dynamical properties of the Galactic halo.

A necessary prerequisite for the completion of the primary goal is the development and evaluation of new technologies for making astrometric observations, particularly CCDs. These devices offer high quantum efficiency, exceptionally low intrinsic noise, and large integration capacity. To date, most astronomical applications of CCDs have concentrated on the measurement of extremely faint objects with only a modest signal-to-noise ratio (SNR). The KPNO 4-m/CCD parallax program uses the CCD in its other limit, that of extremely high SNR observations of bright objects. This application requires both extreme geometric accuracy and long-term system stability—a severe test for any detector system. Because their geometric and photometric properties are determined by their fabrication, CCDs should have accurate and repeatable performance. In particular, CCDs do not rely on electron beam deflection and therefore are immune to many of the difficulties associated with television-type detectors.

In order to be competitive, CCD astrometry must compare favorably with the best photographic programs, such as that of the U.S. Naval Observatory. That program measures single stellar images with a mean error of 23 milliarcseconds and determines parallaxes with mean standard errors of 3.9 milliarcseconds (Harrington and Dahn 1980). Further improvements are expected if fine grain emulsions (van Altena and Mora 1977; Lee and van Altena 1982) and ultraprecise measuring engine technology (van Altena, private communication) are adopted. Therefore, the primary goal of this investigation, the measurement of stellar parallaxes, must await the demonstration that a CCD detector attached to a ground-based telescope has the geometric

<sup>a)</sup> Guest Investigator, KPNO. Kitt Peak National Observatory is operated by AURA, Inc. under contract with the National Science Foundation.

precision needed (1) to measure stellar positions with high internal precision, and (2) to verify that no systematic differences exist between this program and others.

This paper is organized in the following manner. Section II describes the CCD, the relevant hardware, and the observing procedure. Section III describes the data analysis. Particular emphasis is given to algorithms used for determination of the stellar positions. Section IV presents the parallaxes and discusses particulars of the solutions. Section V presents the conclusions and outlines the future of the program. An Appendix gives finding charts and coordinates for six parallax star fields that can be used as geometric standards for detector development.

## II. INSTRUMENTATION AND OBSERVING PROCEDURE

The KPNO 4-m/CCD parallax program uses currently available KPNO User Instruments. No special purpose astrometric instruments were built, nor is there any special preparation done to the telescope or CCD detector before an observing run. At the time the program started, there was only one CCD camera available for the 4-m, that using the Fairchild CCD-211 (Marcus *et al.* 1979, hereinafter referred to as MNL). Since that time several other CCD cameras have become available, but the parallax program still uses the CCD-211 in an attempt to avoid discontinuities. Although the CCD-211 is primitive by current standards, its excellent geometric and photometric performance makes it attractive for this application.

All observations are taken with the following configuration. The CCD camera is placed at the prime focus of the KPNO 4-m telescope behind the doublet corrector (scale = 19.65 arcseconds per millimeter). An intensified television camera is mounted next to the CCD dewar. The optical axis is between the CCD and the TV camera; each is approximately 25 millimeters off-axis. The TV system is used for field acquisition and for automatic guiding. All astrometric observations are taken through the Video Camera "R" filter (2mm OG570 + 2mm KG3 + 2mm quartz). Because the filters are far from the focal plane (about 50 millimeters in the  $f$ -2.7 optical system), special astrometrically flattened filters are not needed. The CCD and its associated dewar have not changed since MNL. Data are recorded on disk and magnetic tape in the console room. Multi-tasking FORTH allows the user to simultaneously take exposures, copy data from disk to tape, and to examine frames on a video display. Guiding is done by the "Leaky Guider." Details of the entire system are found in MNL, the KPNO Facilities Manual (Goad 1982), and the KPNO *Prime Focus CCD Users Guide* (Schoening 1982).

The success of the parallax program depends on many properties of the CCD detector. As mentioned previously, the CCD-211 is primitive by current standards, but it has the following advantages.

(1) In comparison with other currently available CCDs, the CCD-211 has remarkably uniform response. Excepting the large feature seen at wavelengths longer than 7000 Angstroms and the pixels around the perimeter, the device has better than 3% linearity before applying flat-field corrections (see MNL for details). After correction, there are only a few nonphotometric pixels and no bad columns. This means that excellent photometric response is routinely available with only crude approximations to flat-field frames. In addition, one can be reasonably sure that the color dependent flat-field corrections are also small. This is important because the parallax stars are usually much redder than the reference frame stars.

(2) The device appears to have exceptional geometric stability. The CCD was not "thinned" during its manufacture. Hence it is geometrically flat. There are no indications of the "ripples" associated with unsupported thinned CCDs nor are there the "fringes" associated with thinned CCDs that are attached to substrates.

Unfortunately, the disadvantages of the Fairchild CCD-211 outweigh its advantages for most astronomical applications. Indeed, the parallax program suffers from some of the following disadvantages.

(1) The format of the device is only  $190 \times 244$  pixels. Because of its small size, it has a field of view of about 1.2 arcminutes at the prime focus of the KPNO 4-m telescope. This imposes extreme constraints on finding suitable reference fields around the program stars.

(2) The pixels are neither square nor are they on a square lattice. Their nominal size is  $14 \times 18$  microns and they are placed on  $30 \times 18$  micron centers. The rest of the device is taken up by the shift registers, which are covered by an aluminum mask. Because the pixels are not square and not contiguous, special image processing algorithms are required.

(3) Because of its thickness, the device is an excellent detector of cosmic rays. The rate is about 1 event per minute somewhere on the detector (MNL) and each cosmic ray event obliterates the astronomical information in at least 10 pixels. The observing program and data analysis software must account for this problem. Thinned CCDs are also sensitive to cosmic rays, but their construction causes the detection to be limited to a single pixel.

(4) The wavelength range for high precision applications is limited. The CCD has little sensitivity to light shortward of 4500 Angstroms. The intrinsic response of the device changes rapidly at wavelengths longer than 7000 Angstroms (MNL). While these are not problems for the parallax program, they are major limitations for a general purpose observatory instrument.

(5) The device has relatively low quantum efficiency. The pixels have a peak sensitivity of about 25% (MNL) but one must correct this figure for the area of the chip lost to the shift registers. The effective quantum efficiency is approximately 15%. CCDs for other manufactures have upwards of four times this sensitivity.

Since the start of the program (July 1980), the celestial orientation of the CCD has changed by 180 degrees. This was caused by the evolving hardware configuration of the Prime Guider assembly. In 1980 the columns pointed East/West. From 1981.0 to 1982.5 the columns pointed North/South. Since 1982.5 the columns have pointed East/West but are 180 degrees from their original orientation. This rotation has both advantages and disadvantages.

(1) Because the charge stored in the CCD is shifted in particular directions, certain types of charge transfer imperfections cause image shape to be a function of position on the CCD. Many charge transfer problems are functions of the background sky level or the star brightness. To the limit of the accuracy of the parallax solutions presented in Sec. IV, there appears to be no CCD-dependent problems in mapping the frames taken at the various epochs to a common frame. Therefore, the charge transfer properties of the CCD have not changed substantially since MNL. Indeed, rotation of the detector is a powerful tool for the verification of the properties of any CCD device during testing.

(2) Because the CCD-211 has neither square pixels nor a square format, the changing celestial orientation of the detector causes great observational difficulties. In the small field of view, many parallax candidates have only a few adjacent field stars that can serve as a reference frame. It is frustrating to lose a good reference star at a particular epoch because of the rectangular format of the CCD. Many stars that could have had parallax solutions do not because of the different reference frames from 1981.0 to 1982.5. The small format makes field positioning critical. Curious sampling difficulties arise from the peculiar format of the pixels and shift registers. The pixels are spaced at 0.60 by 0.36-arc-second intervals. When the seeing is good, the star images are only marginally oversampled in the direction across the columns but are well sampled along the columns.

The observations of each star at each epoch consist of a sequence of six 2-min integrations. Multiple integrations are necessary to combat the cosmic ray problem. The 2-min exposure is adequate for stars in the 15th–18th magnitude range, although image streaking (a charge transfer nonlinearity that occurs when pixels contain too much charge) may be present for the brightest program stars on nights of both good seeing and good transparency. With this procedure, observation of about 3.5 stars per hour is possible. This figure includes setup, acquisition, offset, integration, and readout times. The data from the CCD were recorded on computer tape and disk. The tape copy forms the observing archive. The disk copy can be displayed in “real-time” so that the quality of the data can be monitored. Telescope focus is always a cause for concern, and its change must be detected and corrected immediately. Because no equivalent to a knife edge focusing test is available for the CCD, focus can only be established by examination

of a sequence of images taken through focus and selecting the best one. The technique is time consuming, and can be profoundly influenced by variable seeing.

Because of the photometric excellence of the CCD-211, only modest efforts were made to obtain flat fields. Routine flat fields are taken from (1) projector illumination of the dome, (2) the flat field projector in the Prime Guider, or (3) moonlit clouds. These three sources produce similar results for most observations. A small residue of the long wavelength photometric depression is seen on frames taken through moonlit clouds when flattened with projector flats. This is attributed to the long wavelength transmission properties of the VCAM “R” filter. Such data frames were of little use for other reasons. Since photometric response of the CCD was seen to be stable over long periods of time, mean flat fields were computed from the individual frames at six-month intervals. These mean flat fields were used for the results presented in Sec. IV. Bias and dark frames were recorded, but they contain no significant features and were not used.

### III. TECHNICAL DETAILS

The CCD hardware reached a stable configuration by late 1980 and has worked reliably since then. The software has arrived at a stable configuration only recently and is still under active development. The analysis of CCD data presents two distinct problems. The first is how to cope with the huge amount of digital data that is produced. Photographic plates form their own archive: their digital representation can be created, analyzed, and destroyed without compromising the archive. The second problem is how to adequately treat the extremely high SNR data produced by the CCD. Inadequate data analysis can obviate any improvement in detector technology.

#### *a) The CCD and Related Matters*

Because of the extreme precision needed to do astrometry, some of the technical CCD details presented by MNL need further discussion. Perhaps the most important are device noise and linearity. As reported in MNL, the dark count rate is about 10 electrons/minute in each pixel. The overall system can be characterized by an equivalent noise of 20 electrons. Although the linearity of the device has been demonstrated to levels of 250 000 electrons per pixel, the onset of subtle charge transfer inefficiencies is believed to occur near half that level.

Because of possible charge transfer problems, the observing procedure limited the brightest image to have about 70 000 electrons per pixel in its core. Because of the broad bandpass of the VCAM “R” filter, the dark night sky contributed about 500 counts per pixel. Because the parallax program did not observe during “dark time,” typical sky background is more nearly 1000 electrons/pixel. Hence, dark and readout noise are insignificant. The practical upper limit for background noise is near 10 000 electrons per pixel. Frames taken

with higher backgrounds (extreme twilight or proximity to the moon) were found to be of extremely low weight in the astrometric mapping solutions.

Figure 1 shows five examples of good CCD frames of the field around vB10 and a U.S. Naval Observatory photograph for comparison. The best of the frames were taken on nights that the telescope operator judged the seeing to be "1 second." The size of the CCD pixels can be inferred from the smallest features on the CCD frames or by noting the size of the 2-pixel blemishes seen on some frames. Because the CCD pixels are not square, the CCD frames in Fig. 1 were repixelized by a bicubic spline interpolator, and are therefore of much poorer quality than the raw data. The seven brightest stars and vB10 were routinely measured. vB10 itself is a typical bright star image while a typical faint reference star would correspond to about the 10th–15th brightest star seen in the field. Typical faint reference stars have about 20 image pixels while the bright ones cover more than one hundred. The windowing of the digital data does not show much of the wings of the stellar images or the photon noise in the sky.

Comparison of our results with theoretical expectations is difficult. Most theoretical discussions of the astrometric performance of solid state detectors (e.g., Chiu 1980; King 1983) make several simplifying assumptions about the image shape. Our experience is that the seeing, telescope focus, and guiding all combine to provide complicated image shapes. As can be seen in Fig. 1, small changes in seeing can change the blending of adjacent stellar images. Frames taken in poor seeing (greater than 2.5 s) cause severe problems in fields as crowded as that around vB10. In view of these difficulties, we feel that the performance of the CCD-211 does not limit the accuracy of the results. Excepting a few frames taken in the best seeing (discussed in Sec. IV), there are no detectable charge transfer irregularities or deviations from the photometric linearity presented by MNL. The analysis of wide variety of image shapes encountered during the two years of observing apparently determines the astrometric accuracy of the CCD-211.

#### b) Image Data Processing

The data were processed in the following manner. Because there are no significant features in the bias frames and negligible dark counts in 2-min exposures, normal bias and dark processing was not needed. Hence, the raw data needed only correction for instrumental electrical offset and flat field response. Once the data were corrected for instrumental response, a two-step process was used for further processing. The first step used an interactive graphics and image display package to extract subrasters around each star. The second step was to compute the star positions. This approach was needed because of the limits on available computer disk space and access to the interactive image display terminal. Archives are kept of the raw data frames, the corrected data frames, and the extracted subrasters.

Development of an optimal algorithm for the computation of image centers was critical to the success of the program. In the following discussion, it must be remembered that these conclusions are based on analysis of our data and may not be generally applicable. Many algorithms were investigated and rejected. Analysis of 1-dimensional marginal distributions (Auer and van Altena 1978) is inadequate because the correction for photo-metrically "bad" pixels requires interpolation and working in crowded fields is difficult. Standard 2-dimensional Gaussian fitting procedures (Auer and van Altena 1978) require major modifications when the pixels are neither square nor on a square lattice. Many perturbations on that algorithm were tried because a Gaussian was only a poor approximation to the image shape. The introduction of extra free parameters (beyond the five needed for the circularly symmetric Gaussian) improves the goodness of fit estimator but does not necessarily improve the measurement of the image position.

The image center algorithm adopted for this investigation was the following. One assumes that the illumination of the detector by a star is circularly symmetric Gaussian:

$$I(x,y) = A + B \cdot \exp \left[ - \frac{(x - x_0)^2 + (y - y_0)^2}{2\sigma^2} \right].$$

The  $i$ th pixel is assumed to have uniform response across its face and has an effective position bounded by  $(x_{\min i}, x_{\max i})$  and  $(y_{\min i}, y_{\max i})$ . For this investigation, the pixel parameters were taken from the manufacturer's data sheet,  $14 \times 18$  microns on  $30 \times 18$  micron centers. Had this not been adequate, they could have been measured in the laboratory. The expected number of counts in the  $i$ th pixel is

$$\begin{aligned} C_i &= \int_{x_{\min i}}^{x_{\max i}} \int_{y_{\min i}}^{y_{\max i}} I(x,y) dx dy, \\ &= \text{const} * [\Phi(\xi_{\max i}) - \Phi(\xi_{\min i})] \\ &\quad * [\Phi(\eta_{\max i}) - \Phi(\eta_{\min i})], \\ \xi &= (x - x_0)/\sqrt{2}\sigma_x, \\ \eta &= (y - y_0)/\sqrt{2}\sigma_y, \end{aligned}$$

where  $\Phi$  is the Error Function. This integration is done for every pixel. The goodness of fit estimator is given by

$$\chi^2 = \sum_i W_i * (O_i - C_i)^2,$$

where  $O_i$  is the count detected in the  $i$ th pixel after bias, dark, and flat field processing. The weighting function  $W_i$  is usually that given by photon statistics but can be modified to exclude bad pixels, etc. This algorithm is extremely general but is extremely expensive to compute. It provides the most stable definition of the image center of the algorithms tested, and works surprisingly well over the wide range of star image shapes encountered.

The removal of "bad" pixels is a nontrivial problem. Because the fitting function is only a poor approxima-

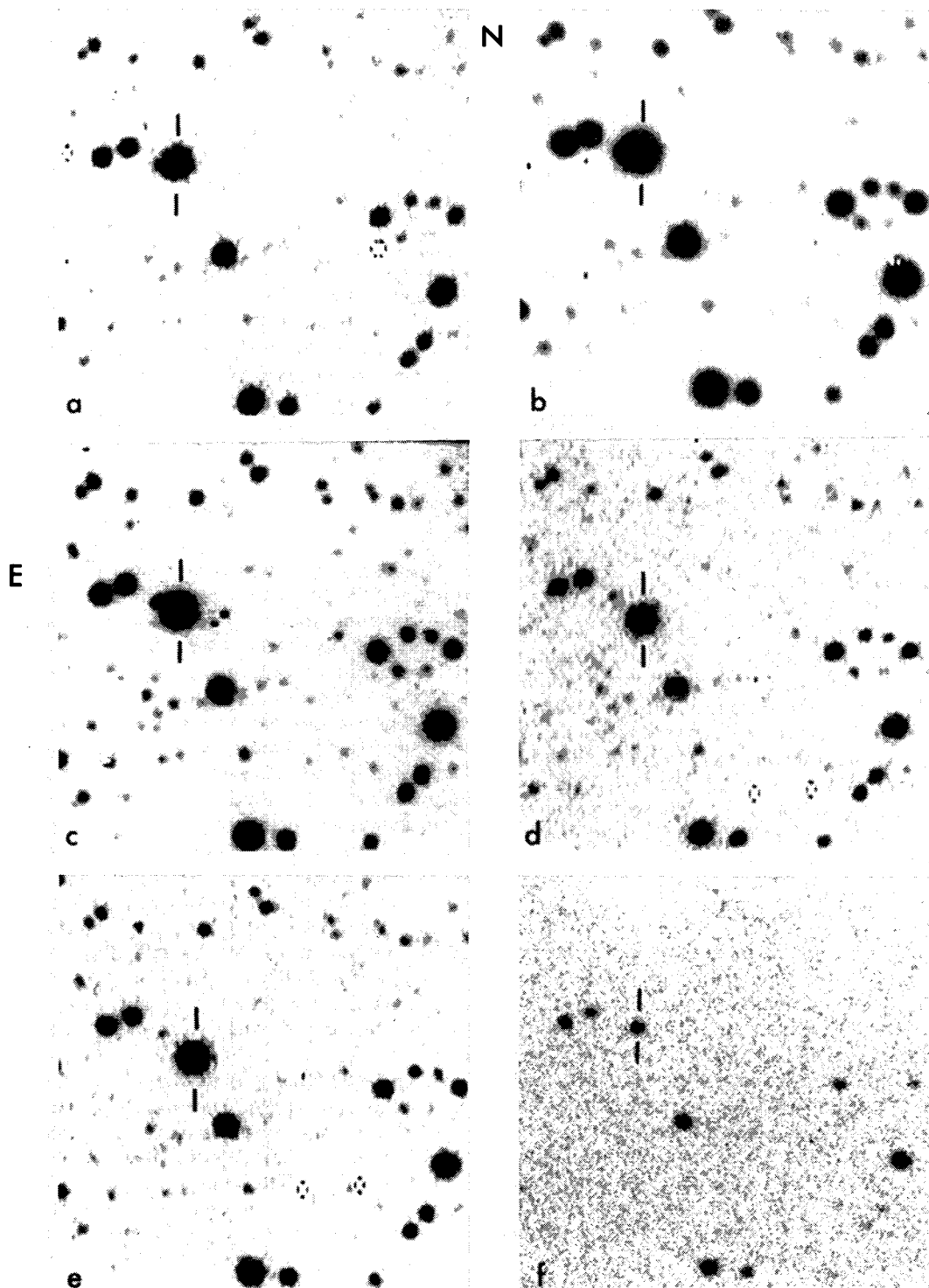


FIG. 1. Panels (a)–(e) show the motion of vB10 observed to date. They also illustrate the limiting magnitude of the 2-min CCD frames and the diversity of the sky conditions. Data from these frames are included in the parallax solution presented in the text. Bicubic spline repixelization algorithm is responsible for image peculiarities near bad pixels, etc. Panel (f) is a 1-hr exposure by the USNO Astrometric reflector with a IIa – D emulsion and GG14 filter.

tion of the actual image shape, one cannot blindly remove all residuals larger than some fiducial value. The following scheme was found to be adequate. The fit included all pixels for the first three iterations. After the third iteration, the list of residuals is sorted in order of increasing absolute value and was normalized by the current value for the standard deviation of the fit. For the  $N$  pixels involved, the difference between the  $(i + 1)$  and the  $(i)$  element is evaluated. If this difference is larger than some threshold value, the  $(i + 1)$  through  $(N)$  image pixels are removed from the fit. The threshold value was taken to be 5, but its precise value is not critical as long as it precludes chopping statistically probable residuals. No further pixel chopping is allowed regardless of the number of iterations needed for convergence. This differential criterion has the advantage that no pixels will be chopped as long as the distribution of residuals is smooth. Systematically large residuals, such as those in the image cores, are retained, while cosmic ray events or nonphotometric pixels are usually removed.

As with all iterative nonlinear least-squares-fitting procedures, an initial estimation of the fitting function is needed. This first guess must compute shape, size, and background, and must not be confused by image crowding and bad pixels. Extremely inaccurate first guess solutions can preclude iterative improvement. The algorithm used for this investigation started with simple image moment analysis followed by image gradient analysis to determine the various parameters. Once the image was located, a search was made for possible adjacent images and bad pixels. These were removed and the image parameters were then recomputed. Even with this elaborate process, many first guesses were so bad that iterative improvement failed. This portion of the code is still under active development.

### c) Astrometric Mapping

The astrometric mapping solution used for this program was based on the standard 2-step iteration technique of alternately computing mean places and then mapping solutions. Sophisticated techniques, such as those developed by Eichhorn and Jefferys (1963), were not needed. Combination of each night's frames (usually six) into nightly means was an unnecessary step. These nightly mean positions were far too sensitive to a single poor measure caused by a cosmic ray event, etc. Despite the many available terms in the code, only the linear terms were significant. The higher order terms and radial terms used by Chiu (1977) were not needed, presumably because the field size is so small.

Perhaps the greatest source for error in the parallaxes presented in Sec. IV comes from differential color refraction. Because the KPNO 4-m telescope is a national facility, the amount of observing time available to a single program is minimal. Hence, it was necessary to do most of the observing away from the meridian. Because the program stars are generally far redder than their

refraction in their apparent positions. Normal practice (van Altena 1971) is to apply a photometric correction to the observed positions. Unfortunately, available data are not adequate to formulate corrections by this method. Instead, the refractive displacement term was included in the same least-squares solution that solved for mean coordinate, parallax, and proper motion. In general, this method is dangerous because there is some correlation between hour angle and parallax factor. However, the three prime candidates discussed in Sec. IV (vB10, LP750-28, and LP750-29) had extensive material at many parallax factors and hour angles. On several nights, these fields were observed at many hour angles in an attempt to break the hour angle-parallax factor correlation and to separate instrumental positional uncertainties from those caused by variable seeing, image shape, telescope focus, etc. The present solutions adequately treat refraction; however, future solutions may be done using photometrically derived corrections.

## IV. PARALLAXES

The observing list was drawn primarily from the LHS (Luyten 1979). Stars were selected for extreme red color, faint apparent magnitude, large proper motion, and availability of a reference frame. The lack of an adequate reference frame within the 1.2-arcmin field of the CCD caused the rejection of many potentially interesting stars. Three additional stars, all discovered by Luyten, were suggested by Liebert (private communication) and Cudworth (private communication). They are LP750-28, LP750-29, and LP251-35. Calibration and interprogram comparison fields are difficult to find at the magnitude and precision expected for this program. Most traditional parallax program standards are 5–10 mag too bright. The only stars with reliable parallaxes determined by the U.S. Naval Observatory (Harrington *et al.* 1983) that are accessible to this program are vB8 (= LHS429) and vB10 (= LHS474). Three stars (vB10, LP750-28, and LP750-29) were given high observing priority because of their extremely rich reference frames.

After the analysis of all available frames, the 81 stars observed to date were divided into three categories. The first contains the 25 stars that have been observed one or more times but do not have adequate reference frames. Table I lists these. The second category contains the 45 stars with good or marginally acceptable reference frames but do not have enough observations to allow computation of a preliminary parallax. These stars are listed in Table II. Unfortunately, the reference fields for many program stars often rely on particularly bright or faint reference stars. The decision to retain or delete these program stars, marked with an asterisk (\*) in Table II, awaits more observations taken on dark nights with good seeing. The third category contains 11 stars that have adequate observational material for the computa-

TABLE I. Stars with unacceptable reference frames.

|         |          |         |
|---------|----------|---------|
| LHS334  | LHS342   | LHS358  |
| LHS515  | LHS523   | LHS542  |
| LHS1294 | LHS1299  | LHS1396 |
| LHS1443 | LHS1451  | LHS1480 |
| LHS1604 | LHS1660a | LHS1670 |
| LHS2034 | LHS2172  | LHS2502 |
| LHS2645 | LHS2930  | LHS3307 |
| LHS3684 | LHS3768  |         |
| LHS5042 | LHS5047  |         |

tion of a preliminary parallax. The solutions for these stars are presented in Table III.

#### a) Preliminary Parallax Solutions

The three prime candidates, vB10, LP750-28, and LP75-29, have enough material that one can be reasonably assured that the determined parallax and its associated uncertainty estimator do not critically depend on a single night's observations. These solutions, which include both refraction and parallax terms, are numerically stable and are presented at the top of Table III. The remainder of Table III presents preliminary parallaxes for eight stars. These latter solutions are based on a minimal amount of data. In general, they rely heavily on a single night's observations taken near one extremum of the parallactic ellipse. In addition, the terms in parallax and refraction are usually so correlated that solutions

TABLE II. Fields awaiting further observations.

|            |           |           |
|------------|-----------|-----------|
| LHS191     | LHS192    | LHS231 *  |
| LHS330 *   | LHS453 *  | LHS483    |
| LHS1074 *  | LHS1420 * | LHS1564   |
| LHS1691    | LHS1970   | LHS2026 * |
| LHS2045 *  | LHS2100   | LHS2110   |
| LHS2112 *  | LHS2174 * | LHS2397 * |
| LHS2554 *  | LHS2828 * | LHS2924 * |
| LHS3061 *  | LHS3168   | LHS3178 * |
| LHS3181    | LHS3259   | LHS3332   |
| LHS3339 *  | LHS3390   | LHS3406   |
| LHS3409 *  | LHS3480   | LHS3548   |
| LHS3683    | LHS3785   | LHS3868 * |
| LHS3933 *  | LHS3954 * | LHS3958 * |
| LHS3973    | LHS4057   |           |
| LHS5046 *  | LHS5062 * |           |
| LP251-35 + |           |           |

#### Notes:

\* Denotes Marginally Acceptable Field Which May Later Prove Unacceptable.

+ Discovered by Luyten (private communication).

including both terms are numerically unstable.

Table III lists both the uncertainty in the mean coordinate and the proper motion and its uncertainty estimator for both the  $X$  and  $Y$  coordinates. The coordinates uncertainty is the dispersion in the mean coordinate as determined from the ensemble of observations. Table III also presents the refraction and parallax terms in the  $X$  coordinate. Owing to the paucity of data and the difficulties associated with the method for removal of atmospheric refraction displacements, the  $Y$  coordinate parallax solutions have been omitted. The uncertainties are substantially larger than for the  $X$  coordinate solutions and usually fail simple tests of numerical stability. The  $X$ -axis refraction solution is denoted by  $r(x)$  and has units of milliarcseconds per unit change in projected tangent of the zenith distance. The coordinate system is aligned so that the  $X$  axis points to the East and the  $Y$  axis points to the North. Unless otherwise noted, the solutions with no  $r(x)$  term listed in Table III are computed with only the parallax term in the solution. The effect of refraction on the measured parallax is unknown. Further observations will resolve this degeneracy. Comments on the individual stars follow.

LP750-28: Some of the 1982.6 observations are systematically displaced from the rest. The listed solution excludes these. If included, the uncertainty for the parallax increases to 3.9 milliarcseconds, but the value computed for the parallax does not change significantly. Further discussion is presented in Sec. IV *b*.

LP750-29: The listed solution includes all 1982.6 observations.

vB10: Some of the 1982.6 observations are systematically displaced from the rest. The listed solution excludes these. If included, the uncertainty for the parallax increases to 3.5 milliarcseconds, but the value computed for the parallax does not change significantly. Further discussion is presented in Sec. IV *b*. The close proximity of vB10 to a faint field star (see Fig. 1) appears to have no effect on the computed center. Figure 1 shows five CCD and one photographic image of the vB10 field. It illustrates the annual motion, the faint and apparently negligible field star that was close to vB10 in 1980, and the variety of sky conditions encountered by the program. The data from each of the CCD frames shown in Fig. 1 were included in the astrometric solution.

LHS 205a: The available observations are of uniformly poor quality. Fitting refraction instead of parallax finds  $r(x) = -21.6 \pm 13.7$ .

LHS 1405: Fitting refraction instead of parallax finds  $r(x) = -3.9 \pm 5.9$ .

LHS 1625: The solution is numerically fragile as only a 4-reference star frame was available at all epochs. Fitting refraction instead of parallax finds  $r(x) = -41.2 \pm 11.8$ . More observations are needed on nights of good seeing to increase the number of reference stars.

TABLE III. Preliminary parallax solutions.

| Star      | Coordinate<br>Uncertainty<br>[mas, Notes 1,2] | Proper Motion<br>$\mu(x)$<br>[mas/year] | $\mu(y)$      | Parallax<br>$\pi(x)$<br>[mas, Note 3] | Refraction<br>$r(x)$<br>[mas, Note 4] | Np | Ne | Nt   |
|-----------|---|---|---------------|---------------------------------------|---------------------------------------|----|----|------|
| LP750-28  | (1.6) (1.0)                                   | -232.7 (2.5)                            | -868.5 (2.9)  | +14.3 (2.5)                           | 20.6 (2.4)                            | 51 | 9  | 1339 |
| LP750-29  | (1.4) (1.0)                                   | -258.9 (2.5)                            | -775.2 (3.3)  | +10.2 (2.2)                           | 0.8 (2.5)                             | 61 | 9  | 1012 |
| VB10      | (0.8) (1.0)                                   | -623.9 (1.8)                            | -1347.9 (2.0) | +178.9 (1.8)                          | -90.2 (2.5)                           | 60 | 9  | 1099 |
| LHS 205a  | (4.9) (4.9)                                   | +458.2 (7.3)                            | -900.4 (7.4)  | +5.1 (5.9)                            |                                       | 34 | 6  | 250  |
| LHS 1405  | (2.9) (3.1)                                   | +581.1 (4.3)                            | -373.6 (3.5)  | +5.9 (3.3)                            |                                       | 37 | 4  | 612  |
| LHS 1625  | (3.5) (4.3)                                   | +320.7 (4.9)                            | -391.8 (6.1)  | +14.9 (3.7)                           |                                       | 40 | 6  | 252  |
| LHS 1625a | (3.5) (4.5)                                   | +359.9 (3.3)                            | -392.2 (3.5)  | +30.6 (3.9)                           |                                       | 35 | 3  | 153  |
| LHS 1742a | (3.1) (2.9)                                   | +768.3 (4.5)                            | -304.8 (4.1)  | +20.6 (3.5)                           |                                       | 29 | 5  | 287  |
| LHS 3481  | (3.1) (3.3)                                   | -273.4 (2.7)                            | -498.3 (2.9)  | +6.5 (5.5)                            |                                       | 30 | 4  | 339  |
| LHS 5356  | (1.6) (1.4)                                   | +235.8 (1.6)                            | +441.6 (1.6)  | +8.6 (2.9)                            |                                       | 36 | 4  | 600  |
| VB 8      | (3.1) (2.9)                                   | -829.3 (4.9)                            | -879.6 (4.3)  | +161.3 (3.7)                          | -100.0 (13.7)                         | 29 | 4  | 163  |

Notes:

- 1) 1 mas = 1 milli-arcsecond. Quantities in parenthesis ( ) are one standard deviation.
- 2) Coordinate Uncertainty is one standard deviation of the parallax star's mean position.
- 3) Listed parallax is relative (uncorrected for the mean parallax of reference frame).  
Y-direction parallax solution is substantially less accurate and are omitted.
- 4) Unit of  $r(x)$  is mas/projected tangent (Zenith Distance). See text.
- 5) Np is the number of individual 2-minute frames included in the solution.  
Ne is the number of distinct epochs (separated by 1 month or more).  
Nt is the number of star measures in the solution.  
The parallax star is measured on every frame. Not all reference stars are measured on every frame.

LHS 1625a: Fitting refraction instead of parallax finds  $r(x) = -158.8 \pm 19.6$ . All observations were taken near the meridian, but there is only one epoch available at large negative parallax factor.

LHS 1742a: To use all available data, a close pair must be included in the reference frame. Hence, the dispersion is somewhat larger because of occasional 50-milliarcsecond residuals for the fainter star of the pair. Fitting refraction instead of parallax yields  $r(x) = -47.0 \pm 7.8$ .

LHS 3481: The reference frame solution seems stable. The anomalously large uncertainty estimator for the parallax probably arises from the extreme red color of the star and its large zenith distance when observed from KPNO. Fitting refraction instead of parallax finds  $r(x) = +17.6 \pm 15.7$ . This appears to be a case where both parallax and refraction terms are present.

LHS 5356: Fitting refraction instead of parallax finds  $r(x) = +43.1 \pm 11.8$ .

vB8: All observations taken on the meridian except 1982.66. Omitting those, solution yields  $p(x) = 161 \pm 3.5$  milliarcseconds. Therefore, parallax and refraction terms are uncoupled in the listed solution.

#### *b) Discussion of the Solution*

Despite the large quantity of data obtained for the systems presented in Table III, there is still a disquieting disagreement in the accuracy of the determined parallaxes when the solutions are taken as an ensemble. The most important factors in the quality of the solution are the astronomical seeing and the level of the sky background on each of the frames. Bad seeing has three detrimental effects. First, the images are larger. This means that the brightness gradient is shallower and that centering is more difficult. Second, the signal-to-noise ratio in a single pixel is lower. In practice, this means that reference stars that are marginal in good seeing are unusable in bad seeing. Because of the small CCD field of view, the loss of these stars precludes using such frames in the astrometric solution. Third, poor seeing will blend otherwise well separated images. High accuracy deconvolution of these images has yet to be attempted. Simple image pixel chopping does not save blended images.

To make matters worse, particularly good seeing causes difficulty as well. The pixels of the Fairchild CCD-211 at the prime focus of the KPNO 4-m telescope are  $0.28 \times 0.36$  arcseconds on  $0.60 \times 0.36$  arcsecond centers. Extremely good seeing causes coarse image sampling. Hence the centering algorithm must deal with a few high signal-to-noise ratio pixels. The high sky background caused by moonlight or clouds causes difficulties. Although the image shape is often excellent, the signal-to-noise ratio per pixel is reduced. Again, the faintest reference stars are so degraded that they cannot be used, thereby precluding further use of the measurable images.

The solutions presented in Table III can be understood in the following manner. It appears that a single

observation of a good star on a good night yields an image center with an accuracy of about 10 milliarcseconds (0.5 microns). All things being equal, these centers appear to combine according to the laws of Gaussian statistics when used in solutions for parallax, proper motion, and refraction. The 4-m/CCD system has remained stable since the inception of the program in 1980.6, the uncertainty in the mean position scales according to the square root of the number of observations. Gross differences between the various solutions listed in Table III presumably reflect difficulties with the reference frames. When possible, poor seeing and high background data were rejected. Unfortunately, this could not be done when the rejection of data would lose all information about the star at a particular parallactic elongation. As more data become available, poor data will be omitted or given lower weight. The KPNO prime focus hardware configuration may have stabilized and the rotation of the detector may cease. Hence, reference stars near the edge of the detector and not just in the central square can be used.

An approximation to a fiducial test of the CCD itself can be constructed from the observations taken to isolate the refraction and parallax terms. When possible, particularly interesting stars such as vB10 were monitored as they rose or set. The nightly proper motion is small compared with currently available accuracy and changes in parallax are minute. Refraction is responsible for all significant changes in the apparent positions of the stars in the field. Such data can be used to compute refraction corrections for each of the stars. Since image shape remains constant on a good night, the interaction between the image centering algorithm and the shapes of the images stays the same. The only variable is the placement of the stars on the CCD. Intercomparison of these frames tests CCD dependent uncertainties in image position. When these solutions were done, 4–6 milliarcsecond positional uncertainties were found. This figure is either limited by photon statistics or by the inherent geometrical properties of the CCD or both. The typical accuracy of 10 milliarcseconds found for the solutions presented in Table III is interpreted as being primarily caused by the centering algorithm's inability to conquer the myriad "cosmic" sources of image degradation.

A disquieting problem appeared in the September 1982 data. For both LP750-28 and vB10, data from some of the nights differed systematically from that taken on the other nights. The difference was up to 50 milliarcseconds and occurred primarily along the column direction of the CCD. The nights in question had exceptionally good seeing and low sky background. Only the parallax star was affected; the reference fields were mapped to typical accuracy. If these frames (6 of 18 for LP750 — 28 and 10 of 22 for vB10) were included in the solution, the uncertainty estimators given in Table III increase by about 40 percent. These data are systematically different from the rest taken at the same epoch and

clearly disagree with the solution computed from more than 60 other frames taken in the preceding two years. These data were omitted from the solution for the following reason. In both fields, the parallax star is the brightest object. In both cases, the displacement is along the column direction of the CCD. The number of counts in the brightest image pixel is dangerously close to that where charge transfer inefficiency is thought to begin. Useful data with about 10% more counts in the brightest pixels were taken early in 1981. It is believed that the onset of charge transfer inefficiency is changing as the device ages. If there is sloppy charge transfer, then the large residuals are explained. Further data will be taken to test this hypothesis.

One aspect of the astrometry that was not recognized until recently is the effect of the known radial distortion of the 4-m telescope. As stated earlier, all solutions are mapped to the common frame using only linear coefficients. Unfortunately, this does not assist in determination of the absolute geometry of the field because the centerline of the CCD has stayed at the same location of the 4-m focal plane for all observations. While the occasional rotation of the CCD around its center yields information about its geometry, no test of the geometry of the scene that illuminates the CCD has been done. The approximate size of the radial distortion is known (*KPNO ASTRO User's Manual*, Hammond 1982). Because the field of view of the CCD is so small, the effect is small but not trivial. Numerical simulations have been done. Synthetic centers based on the nominal radial distortion terms were computed and subsequently analyzed with an astrometric mapping code constrained to use only linear terms. The mapping yielded a rms scatter of 2.5 milliarcseconds. This means that the field can be assumed to be locally rectilinear for applications with a scatter much larger than this. Sophisticated mapping is needed for more precise work. Further observations will be taken to map the correction from chip coordinates, and final results will be transformed to a rectilinear system.

#### V. CONCLUSIONS

Both the primary and secondary objectives of the program have been met. The solutions presented in Sec. IV show that CCD parallax astrometry can be competitive with traditional photographic programs. The mean error for the position of a single star is about 10 milliarcseconds, and all measures were mapped to a common frame using only linear mapping terms. The comparison of the parallaxes of  $\nu$ B8 and  $\nu$ B10 with other values shows that systematic errors are undetectably small at this time. Our value for the absolute parallax of  $\nu$ B10 is  $179 \pm 2$  milliarcseconds. This agrees with the value of  $171 \pm 6$  given by Gliese and Jahreiss (1979) and with  $174 \pm 5$  given by Harrington *et al.* (1983). Other parallaxes for this star refer to its brighter common proper motion companion. The comparison for  $\nu$ B8 is equally good. The USNO value is  $154 \pm 6$  milliarcseconds (Harrington *et al.* 1983), and Gliese (1969) lists  $161 \pm 6$ , and

we find  $162 \pm 4$ . The KPNO 4-m/CCD program is capable of measuring stellar trigonometric parallaxes with extremely small internal and external errors. When taken as an ensemble, the eight preliminary parallax solutions show that the high accuracy seen for  $\nu$ B10, LP750-28, and LP750-29 is not coincidental. The difference in accuracy is explained by the limited access to the 4-m telescope.

The preliminary parallaxes for 11 stars are given in Table III. Of these, eight are considered preliminary because of insufficient observations and possible difficulties associated with the correction for refraction. Two stars with well-determined parallaxes, LP750-28 and LP750-29, are apparently members of the Galactic halo population. Two of the preliminary parallaxes, those for LHS1625a and LHS1742a, are significantly nonzero. Further observations of these systems will be given high priority. Despite their preliminary nature, the eight systems listed in the second part of Table III have parallaxes with internal accuracies equal to typical definitive USNO parallaxes.

The KPNO 4-m/CCD parallax program produces high quality astrometric data with a minimum of cost. A general purpose CCD is used for the detector. No special astrometric instrument such as those developed by Gatewood and Stein (1980) and Jones and York (1982) is needed. For the program stars, a single 2-min integration is of the same astrometric weight as four 1-hr exposures with the USNO astrometric reflector and Ia - D photographic plates measured on SAMM (Harrington *et al.* 1983). Because the data are digitized by the CCD controller, astrometric results can be obtained in almost "real time." Since the astrometric data are obtained quickly, a significant observing program can be done with only a minimal commitment of telescope time.

The authors would like to thank the following persons. Harvey Butcher, Roger Lynds, and James Westphal have provided major scientific and moral support. The computer time provided by Lynds and Westphal was critical to the success of the parallax program. The support of the entire staff of the Kitt Peak National Observatory was appreciated. The talents of the following people made the collection of the observations a pleasant experience: Dan Brodzik, Bill Ditsler, Don Farris, Steve Marcus, Caty Pilachowski, and Dave Stultz. The generous allotments of observing time by the KPNO Telescope Allocation Committee made this program possible. The support of this program by Geoff Burbidge and Dale Schrage is appreciated.

#### APPENDIX

Because of the need for geometric standard fields for detector development and performance verification, the finding charts and coordinate lists for six parallax program fields are presented. The finding charts appear as Figs. A1-A6 and the associated coordinate lists appear as Tables A1-A6. The coordinate system for all fields is as follows. The positive  $X$  direction is approximately

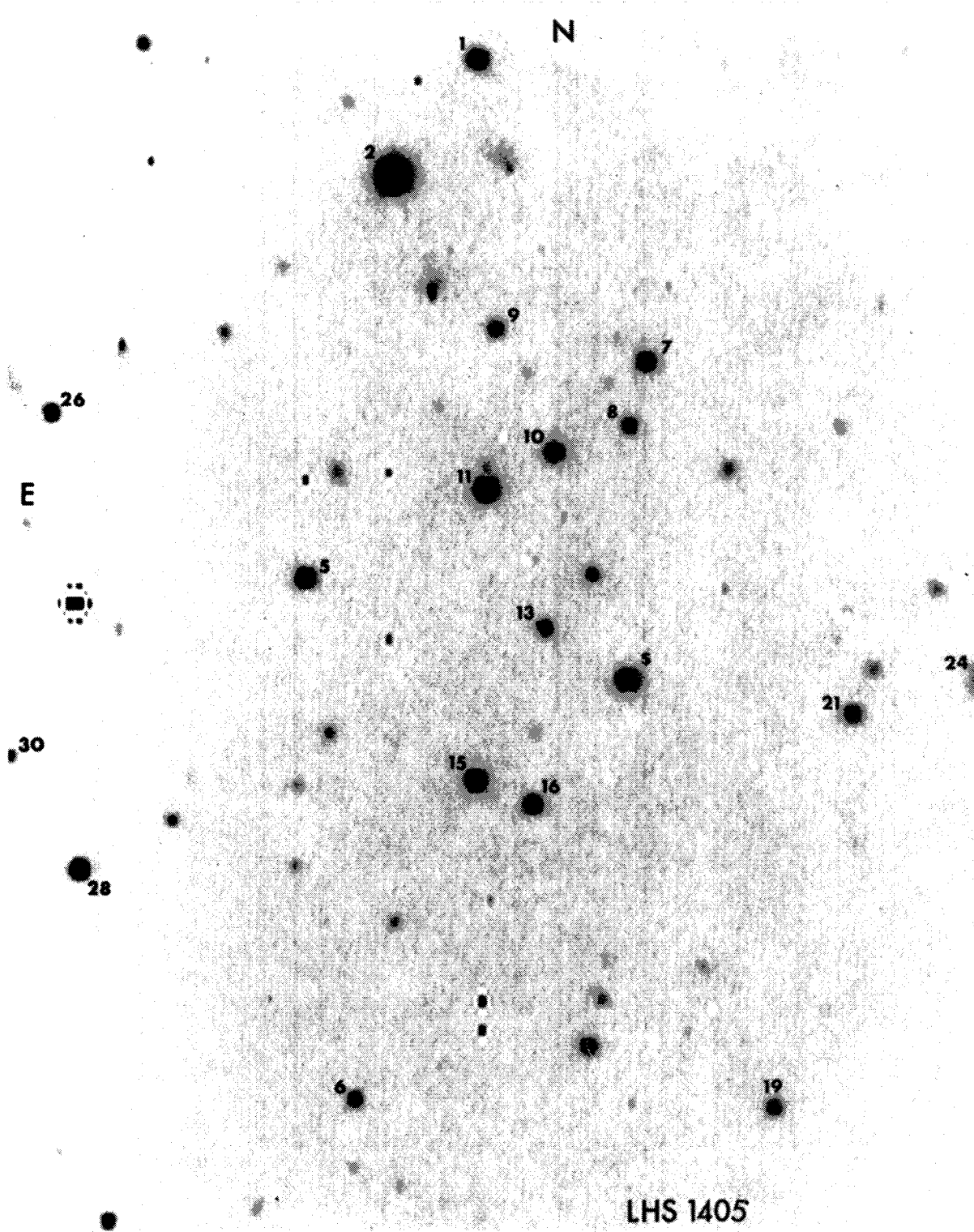


FIG. A1. Finding chart for the field of LHS1405. The numbers refer to the coordinates listed in Table A1. LHS1405 is marked with a S. See text for further details.

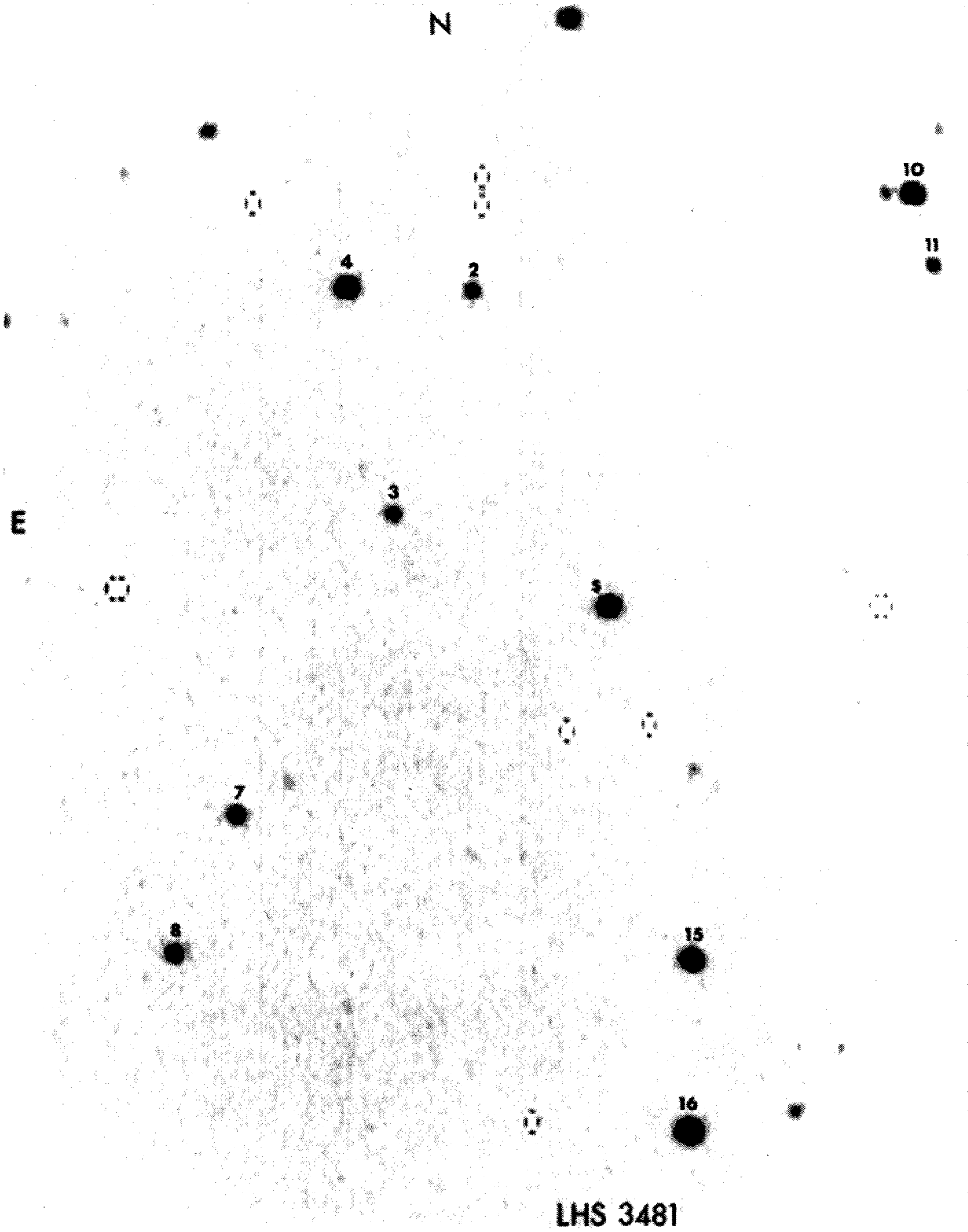


FIG. A2. Finding chart for the field of LHS3481. The numbers refer to the coordinates listed in Table A2. LHS3481 is marked with a \$. See text for further details.

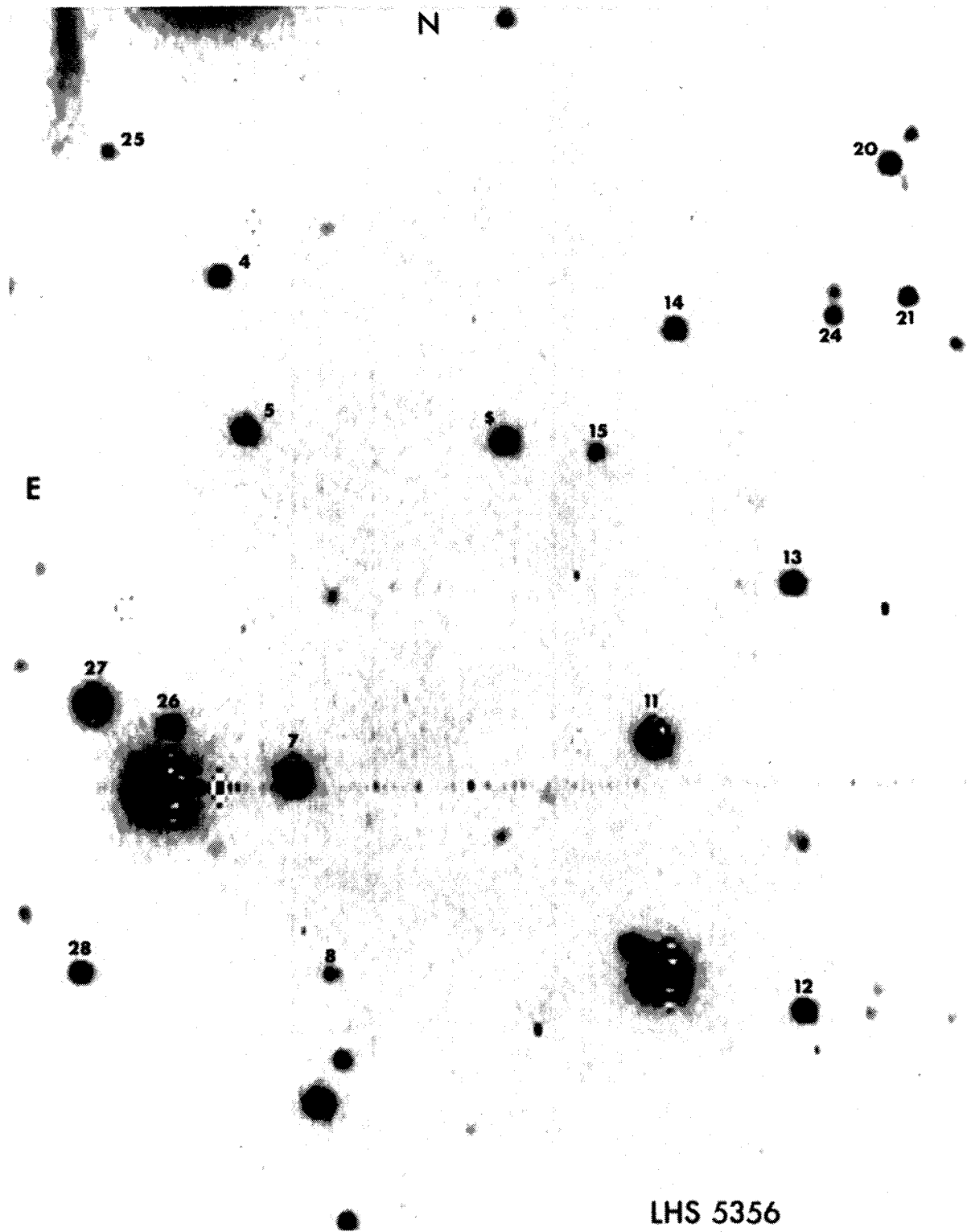


FIG. A3. Finding chart for the field of LHS5356. The numbers refer to the coordinates listed in Table A3. LHS5356 is marked with a S. See text for further details.

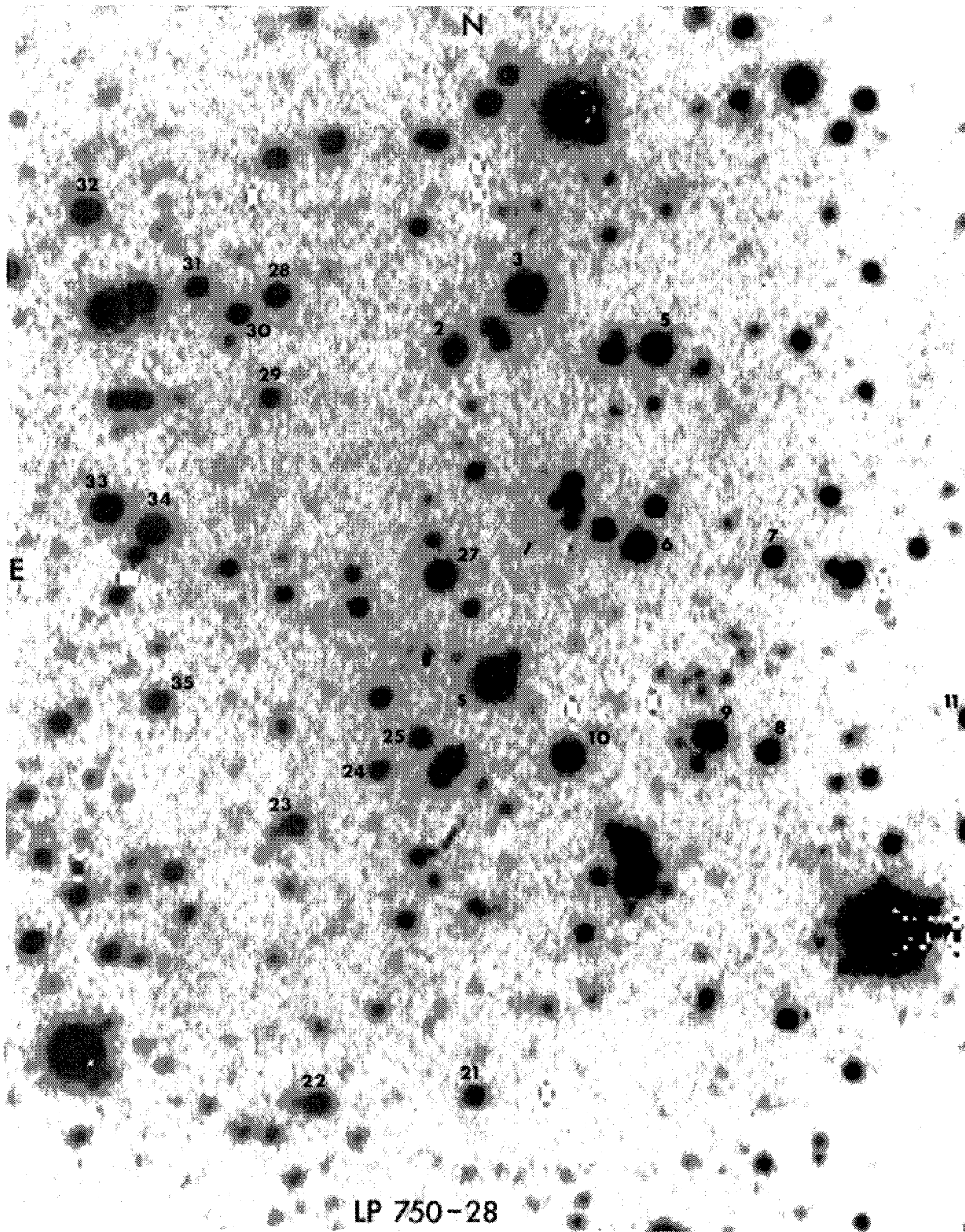


FIG. A4. Finding chart for the field of LP750-28. The numbers refer to the coordinates listed in Table A4. LP750-28 is marked with a \$. See text for further details.

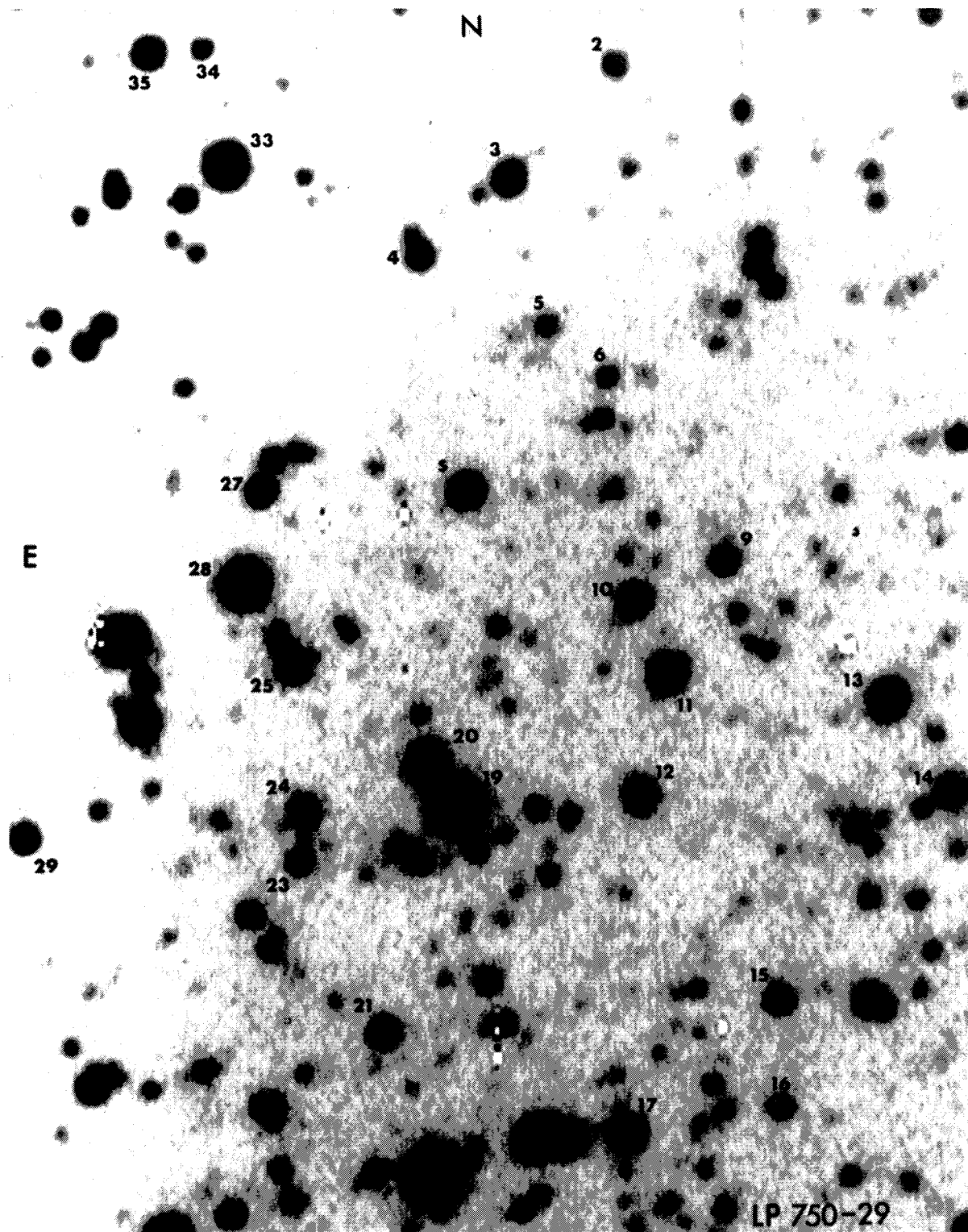


FIG. A5. Finding chart for the field of LP750-29. The numbers refer to the coordinates listed in Table A5. LP750-29 is marked with a \$. See text for further details.

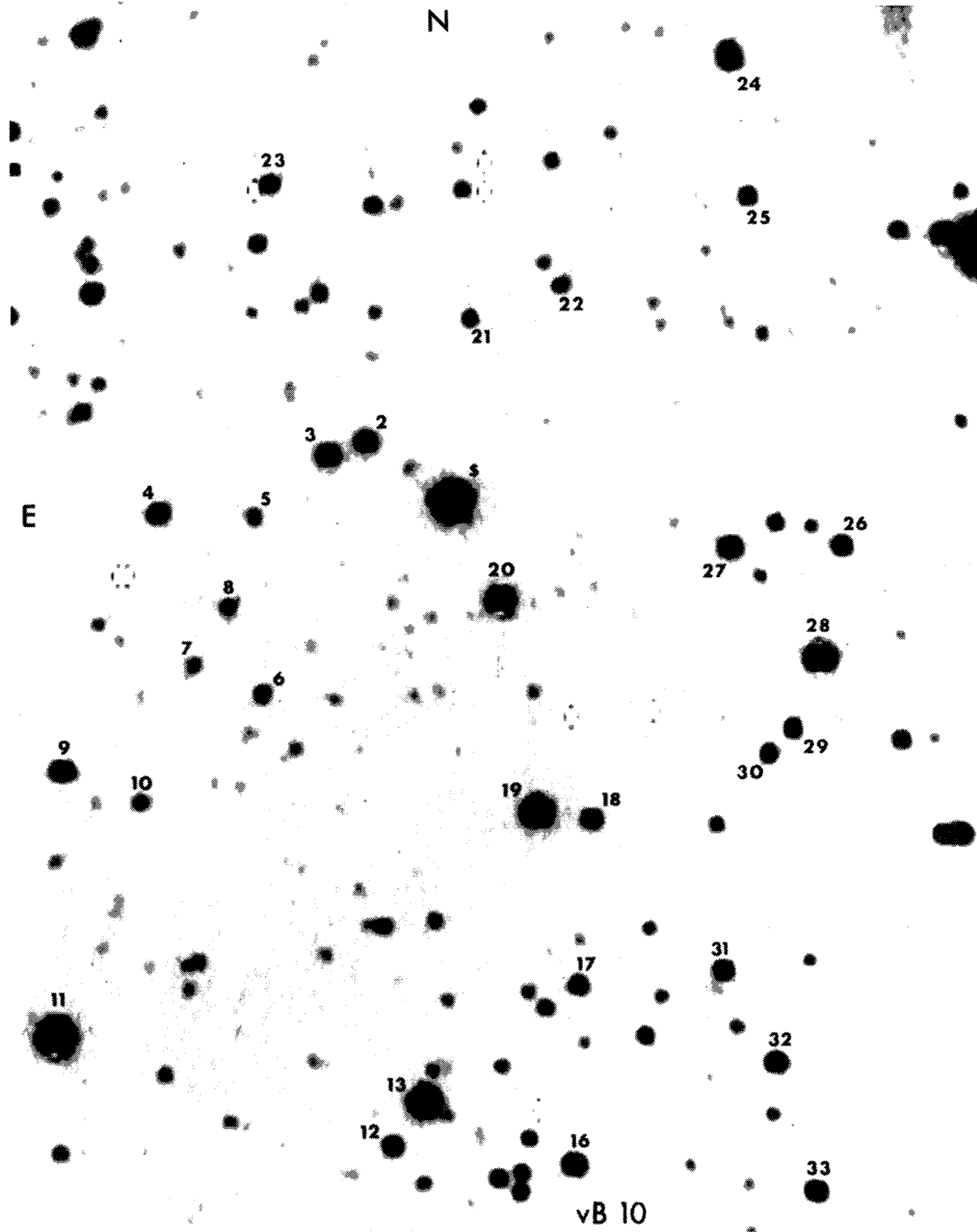


FIG. A6. Finding chart for the field of vB10. The numbers refer to the coordinates listed in Table A6. vB10 is marked with a \$. See text for further details.

TABLE A1. Mean places for the LHS 1405 field.

| Star | X<br>(Coordinate system discussed in text) | Y              | A    |
|------|--|----------------|------|
| 1    | -2140.3 (2.4)                              | 37882.3 (2.5)  | 4.7  |
| 2    | 4580.7 (2.2)                               | 28528.6 (1.8)  | 30.4 |
| 5    | 11837.4 (3.5)                              | -4165.6 (3.3)  | 3.7  |
| 6    | 8047.8 (9.4)                               | -46588.0 (6.1) | 1.1  |
| 7    | -15683.9 (3.9)                             | 13472.1 (2.5)  | 3.3  |
| 8    | -14277.6 (2.7)                             | 8245.3 (3.9)   | 1.8  |
| 9    | -3519.2 (2.9)                              | 16063.0 (2.9)  | 2.1  |
| 10   | -8235.3 (2.9)                              | 6071.7 (3.3)   | 3.8  |
| 11   | -2783.6 (3.9)                              | 3051.1 (2.4)   | 7.4  |
| 13   | -7529.9 (5.1)                              | -8286.7 (5.1)  | 1.3  |
| 15   | -1909.2 (4.3)                              | -20661.3 (2.9) | 4.9  |
| 16   | -6493.3 (2.7)                              | -22604.7 (2.4) | 3.6  |
| 19   | -26033.3 (4.7)                             | -47333.4 (4.7) | 2.0  |
| 21   | -32413.1 (2.9)                             | -15288.0 (3.1) | 2.7  |
| 24   | -43672.3 (2.2)                             | -12340.6 (2.4) | 20.2 |
| 26   | 32428.8 (3.1)                              | 9255.5 (2.9)   | 2.3  |
| 28   | 30293.0 (3.1)                              | -27998.8 (2.7) | 4.4  |
| 30   | 35905.2 (4.9)                              | -18747.6 (4.5) | 1.1  |

TABLE A2. Mean places for the LHS 3481 field.

| Star | X<br>(Coordinate system discussed in text) | Y              | A    |
|------|--|----------------|------|
| 2    | 10127.3 (3.1)                              | 26371.6 (3.7)  | 6.7  |
| 3    | 16280.5 (3.3)                              | 7978.0 (4.9)   | 6.0  |
| 4    | 20369.1 (2.9)                              | -26455.9 (3.3) | 23.9 |
| 7    | 28568.2 (2.2)                              | -16948.9 (4.1) | 10.7 |
| 8    | 33406.4 (2.7)                              | -28311.6 (2.4) | 9.7  |
| 10   | -25551.7 (3.7)                             | 35052.4 (2.4)  | 28.4 |
| 11   | -27334.4 (4.1)                             | 29247.5 (3.5)  | 5.2  |
| 15   | -8676.3 (1.8)                              | -27778.5 (2.2) | 33.4 |
| 16   | -8694.2 (2.0)                              | -41736.0 (2.9) | 52.9 |

TABLE A3. Mean places for the LHS 5356 field.

| Star | X<br>(Coordinate system discussed in text) | Y              | A     |
|------|--|----------------|-------|
| 4    | 30465.5 (1.8)                              | 4013.1 (1.4)   | 16.0  |
| 5    | 28341.8 (0.6)                              | -8680.1 (1.6)  | 45.6  |
| 7    | 24583.1 (1.2)                              | -37189.0 (1.0) | 131.4 |
| 8    | 21529.0 (4.3)                              | -53196.0 (5.9) | 3.4   |
| 11   | -4865.9 (2.9)                              | -34086.8 (2.0) | 149.8 |
| 12   | -16942.2 (1.8)                             | -56194.0 (2.5) | 20.7  |
| 13   | -16265.6 (1.4)                             | -21312.5 (1.6) | 22.0  |
| 14   | -6766.9 (1.8)                              | -487.5 (2.0)   | 16.3  |
| 15   | -298.1 (2.0)                               | -10557.0 (2.2) | 6.9   |
| 20   | -24468.8 (1.4)                             | 12983.6 (1.2)  | 18.4  |
| 21   | -25828.5 (1.4)                             | 2106.6 (3.5)   | 7.9   |
| 24   | -19722.1 (2.4)                             | 607.2 (2.5)    | 7.2   |
| 25   | 39479.5 (4.1)                              | 14423.6 (5.9)  | 3.0   |
| 26   | 34497.8 (1.4)                              | -33036.4 (2.2) | 29.8  |
| 27   | 40829.5 (1.0)                              | -31236.3 (0.8) | 119.3 |
| 28   | 41948.7 (1.4)                              | -53079.9 (1.6) | 15.1  |

TABLE A4. Mean places for the LHS 750-28 field.

| Star | X<br>(Coordinate system discussed in text) | Y              | A    |
|------|--|----------------|------|
| 2    | 5885.1 (2.7)                               | 19413.4 (2.2)  | 11.3 |
| 3    | -0.6 (2.4)                                 | 24283.6 (2.4)  | 53.2 |
| 5    | -10838.6 (2.9)                             | 19652.1 (2.7)  | 21.8 |
| 6    | -9447.2 (2.7)                              | 3128.7 (2.5)   | 17.3 |
| 7    | -20494.3 (4.1)                             | 2270.5 (2.2)   | 4.1  |
| 8    | -20021.2 (2.7)                             | -13984.8 (2.4) | 5.2  |
| 9    | -15154.9 (2.9)                             | -12654.9 (1.6) | 15.1 |
| 10   | -3408.8 (3.7)                              | -14414.0 (2.2) | 24.6 |
| 11   | -36632.8 (2.9)                             | -11067.9 (2.2) | 5.4  |
| 13   | -37711.8 (3.3)                             | -25123.9 (3.3) | 5.1  |
| 21   | 4453.3 (2.7)                               | -42467.5 (2.5) | 5.3  |
| 22   | 17529.5 (3.5)                              | -43133.3 (3.9) | 6.1  |
| 23   | 19312.3 (3.1)                              | -20124.1 (2.9) | 6.1  |
| 24   | 12276.3 (4.3)                              | -15530.6 (3.1) | 3.1  |
| 25   | 8764.7 (8.8)                               | -12965.4 (7.8) | 4.7  |
| 27   | 7032.5 (3.3)                               | 672.9 (2.9)    | 16.9 |
| 28   | 20668.2 (2.4)                              | 24021.8 (2.5)  | 9.3  |
| 29   | 21285.4 (4.3)                              | 15557.1 (2.7)  | 4.3  |
| 30   | 23896.7 (2.7)                              | 22550.2 (3.5)  | 5.1  |
| 31   | 27351.2 (3.3)                              | 24711.7 (3.3)  | 5.1  |
| 32   | 36508.7 (5.5)                              | 31033.1 (2.4)  | 15.0 |
| 33   | 34804.7 (3.3)                              | 6220.1 (2.4)   | 19.8 |
| 34   | 30952.1 (3.7)                              | 4446.8 (2.2)   | 20.4 |
| 35   | 30534.3 (3.9)                              | -10027.0 (2.5) | 6.2  |
| 36   | 32081.7 (2.9)                              | -59006.2 (4.7) | 19.2 |

TABLE A5. Mean places for the LP 750-29 field.

| Star | X<br>(Coordinate system discussed in text) | Y              | A     |
|------|--|----------------|-------|
| 2    | -15042.2 (2.9)                             | 34822.3 (4.1)  | 6.5   |
| 3    | -6265.9 (3.5)                              | 25228.9 (2.4)  | 21.2  |
| 4    | 1208.1 (3.5)                               | 18927.9 (6.5)  | 9.9   |
| 5    | -9279.6 (4.5)                              | 13112.2 (2.2)  | 4.0   |
| 6    | -14206.7 (3.3)                             | 8847.0 (3.3)   | 4.0   |
| 9    | -23813.6 (2.5)                             | -6565.8 (1.8)  | 10.2  |
| 10   | -16293.3 (2.0)                             | -9800.4 (2.0)  | 16.2  |
| 11   | -19005.9 (1.4)                             | -16080.4 (1.6) | 27.9  |
| 12   | -16597.3 (2.4)                             | -26173.6 (3.7) | 12.6  |
| 13   | -37362.5 (2.4)                             | -18369.9 (2.0) | 35.1  |
| 14   | -42554.3 (3.7)                             | -25999.4 (2.7) | 14.7  |
| 15   | -28053.9 (2.2)                             | -43307.4 (3.7) | 9.0   |
| 16   | -28137.8 (4.1)                             | -52309.1 (3.9) | 5.9   |
| 17   | -15339.4 (2.4)                             | -54487.6 (4.3) | 22.4  |
| 19   | -1261.8 (6.1)                              | -27023.9 (6.7) | 10.0  |
| 20   | 1026.8 (2.7)                               | -23365.6 (3.1) | 44.8  |
| 21   | 4853.5 (2.2)                               | -45809.1 (2.7) | 12.2  |
| 23   | 11668.7 (5.9)                              | -31526.8 (8.4) | 6.2   |
| 24   | 11201.0 (2.5)                              | -27267.1 (3.7) | 12.7  |
| 25   | 12037.1 (3.5)                              | -15215.7 (6.3) | 23.4  |
| 26   | 15993.6 (4.3)                              | -8342.9 (6.1)  | 101.2 |
| 27   | 14516.3 (3.9)                              | -543.9 (5.7)   | 15.0  |
| 29   | 34289.6 (2.5)                              | -29483.9 (3.5) | 16.8  |
| 33   | 17054.5 (4.3)                              | 26419.6 (6.7)  | 80.9  |
| 34   | 19005.3 (3.3)                              | 36190.6 (2.5)  | 6.4   |
| 35   | 23340.7 (3.3)                              | 35769.6 (1.8)  | 24.5  |

TABLE A6. Mean places for the vB10 field.

| Star | X                                     | Y              | A    |
|------|---------------------------------------|----------------|------|
|      | (Coordinate system discussed in text) |                |      |
| 2    | 10365.1 (2.4)                         | 29647.5 (1.8)  | 11.2 |
| 3    | 13361.9 (1.8)                         | 28477.2 (1.8)  | 13.8 |
| 4    | 27220.3 (2.4)                         | 23500.2 (2.0)  | 9.8  |
| 5    | 19356.6 (3.3)                         | 23340.9 (3.5)  | 2.1  |
| 6    | 21300.5 (2.5)                         | 15821.9 (3.5)  | 2.9  |
| 7    | 24017.3 (4.3)                         | 10908.2 (4.1)  | 1.8  |
| 8    | 18401.1 (2.9)                         | 8705.5 (2.9)   | 4.0  |
| 9    | 34789.8 (2.5)                         | 2024.9 (1.4)   | 8.5  |
| 10   | 28239.9 (3.1)                         | -396.9 (2.5)   | 2.7  |
| 11   | 34644.6 (3.3)                         | -19544.1 (2.7) | 99.5 |
| 12   | 7159.9 (2.5)                          | -27493.7 (2.4) | 6.9  |
| 13   | 4632.9 (2.5)                          | -23932.4 (2.7) | 51.6 |
| 16   | -7470.9 (3.3)                         | -28637.6 (2.9) | 13.3 |
| 17   | -7631.3 (2.0)                         | -14263.1 (2.0) | 5.5  |
| 18   | -8530.7 (1.6)                         | -839.3 (2.2)   | 9.0  |
| 19   | -4103.3 (1.8)                         | -355.0 (1.6)   | 43.2 |
| 20   | -860.0 (2.0)                          | 16942.8 (1.6)  | 30.4 |
| 21   | 2074.3 (2.9)                          | 39903.1 (2.7)  | 2.8  |
| 22   | -5248.9 (3.5)                         | 42734.5 (3.1)  | 2.5  |
| 23   | 19445.7 (2.7)                         | 45760.5 (2.9)  | 3.2  |
| 24   | -18639.2 (2.4)                        | 61626.9 (3.5)  | 12.9 |
| 25   | -20327.7 (2.2)                        | 50187.0 (2.0)  | 4.3  |
| 26   | -28341.0 (2.0)                        | 21837.5 (2.0)  | 7.1  |
| 27   | -19390.3 (2.0)                        | 21578.0 (1.2)  | 12.5 |
| 28   | -26765.4 (1.8)                        | 12708.4 (1.8)  | 36.8 |
| 29   | -24681.1 (2.2)                        | 6871.8 (3.7)   | 4.3  |
| 30   | -22797.2 (2.5)                        | 4802.8 (2.4)   | 4.4  |
| 31   | -19343.0 (2.0)                        | -12727.7 (2.2) | 7.0  |
| 32   | -23635.4 (1.6)                        | -20075.1 (2.0) | 11.0 |
| 33   | -26981.6 (2.4)                        | -30265.7 (2.9) | 11.1 |

East and the positive  $Y$  direction is approximately North. The alignment is within a few degrees. The coordinates are given in milliarcseconds and are followed by their one standard deviation uncertainty estimators. The absolute scale is probably accurate to about 0.1 percent. Each of the CCD frames has repixelized with a bicubic spline interpolator. This process tends to over-emphasize bad pixels and other minor image irregularities. The amplitude  $A$  listed in Tables A1–A6 is the amplitude of the fitting function and is proportional to brightness. The conversion between  $A$  and stellar magnitudes has not been calibrated.

As mentioned in the text, there is probably a radial distortion term in these coordinates. Simulation of this term showed that if the distortion is ignored when mapping onto a perfect rectilinear coordinate system, then the difference will appear as a rms scatter of 2.5 milliarcseconds. Hence, these coordinates may be used without including a radial term in the transformation for applications with intrinsic dispersions large in comparison with that figure. For precise applications, the telescope optical axis is at approximately ( $X = -490000.0$ ,  $Y = 0.0$ ), and a simple radial term should be sufficient.

## REFERENCES

- Auer, L. H., and van Altena, W. F. (1978). *Astron. J.* **83**, 531.  
 Chiu, L.-T. G. (1977). *Astron. J.* **82**, 842.  
 Chiu, L.-T. G. (1980). *Celestial Mech.* **20**, 191.  
 Dahn, C. C., Harrington, R. S., Riepe, B. Y., Christy, J. W., Guetter, H. H., Kallarakal, V. V., Miranian, M., Walker, R. L., Vrba, F. J., Hewitt, A. V., Durham, W. S., and Ables, H. D. (1982). *Astron. J.* **87**, 419.  
 Eichhorn, H., and Jefferys, W. H. (1963). *Astron. J.* **68**, 71.  
 Gatewood, G. D., and Stein, J. W. (1980). *Bull. Am. Astron. Soc.* **12**, 455.  
 Gliese, W. (1969). *Catalog of Nearby Stars*, Veroff, Astr. Rechen-Inst., No. 22, 1.  
 Gliese, W., and Jahreiss, H. (1979). *Astron. Astrophys. Suppl.* **38**, 423.  
 Goad, J., ed. (1982). *KPNO Facilities Manual* (Kitt Peak National Observatory, Tucson).  
 Hammond, S. (1982). *ASTRO User's Manual* (Kitt Peak National Observatory, Tucson).  
 Harrington, R. S., and Dahn, C. C. (1980). *Astron. J.* **85**, 454.

1983AJ.....88.1489M

- Harrington, R. S., Dahn, C., and Kallarakal, V. V. (1982). *Astron. J.* **88**, 1038.
- Jones, B. F., and York, D. G. (1982). *Bull. Am. Astron. Soc.* **13**, 73.
- King, I. R. (1983). *Publ. Astron. Soc. Pac.* **95**, 163.
- Lee, J.-F., and van Altena, W. F. (1982). *Bull. Am. Astron. Soc.* **14**, 645.
- Luyten, W. J. (1979). *LHS Catalog* (University of Minnesota, Minneapolis).
- Marcus, S. L., Nelson, R. E., and Lynds, C. R. (1979). *Proc. S.P.I.E.* **172**, 207 (MNL).
- Schoening, W. (1982). *Prime Focus CCD Users Manual* (Kitt Peak National Observatory, Tucson).
- van Altena, W. F., and Mora, C. L. (1977). *Bull. Am. Astron. Soc.* **9**, 599.
- van Altena, W. F. (1971). *Astron. J.* **76**, 932.